IOP PUBLISHING JOURNAL OF PHYSICS D: APPLIED PHYSICS

J. Phys. D: Appl. Phys. **42** (2009) 145408 (8pp) doi:10.1088/0022-3727/42/14/145408

Calculations of the resonant response of carbon nanotubes to binding of DNA

Meng Zheng[1], Kilho Eom[2] and Changhong Ke[1]

[1] Department of Mechanical Engineering, State University of New York at Binghamton, Binghamton, NY 13902, USA

[2] Department of Mechanical Engineering, Korea University, Seoul 136-701, Republic of Korea

E-mail: cke@binghamton.edu and kilhoeom@korea.ac.kr

Received 6 April 2009, in final form 1 June 2009
Published 1 July 2009
Online at stacks.iop.org/JPhysD/42/145408

Abstract

We theoretically study the dynamical response of carbon nanotubes (CNTs) to the binding of DNA in an aqueous environment by considering two major interactions in DNA helical binding to the CNT side surface: adhesion between DNA nucleobases and CNT surfaces and electrostatic interactions between negative charges on DNA backbones. The equilibrium DNA helical wrapping angle is obtained using the minimum potential energy method. Our results show that the preferred DNA wrapping angle in the equilibrium binding to CNT is dependent on both DNA length and DNA base. The equilibrium wrapping angle for a poly(dT) chain is larger than a comparable poly(dA) chain as a result of dT in a homopolymer chain having a higher effective binding energy to CNT than dA. Our results also interestingly reveal a sharp transition in the wrapping angle-DNA length profile for both homopolymers, implying that the equilibrium helical wrapping configuration does not exist for a certain range of wrapping angles. Furthermore, the resonant response of the DNA–CNT complex is analysed based on the variational method with a Hamiltonian which takes into account the CNT bending energy as well as DNA–CNT interactions. The closed-form analytical solution for predicting the resonant frequency of the DNA–CNT complex is presented. Our results show that the hydrodynamic loading on the oscillating CNT in aqueous environments has profound impacts on the resonance behaviour of DNA–CNT complexes. Our results suggest that detection of DNA molecules using CNT resonators based on DNA–CNT interactions through frequency measurements should be conducted in media with low hydrodynamic loading on CNTs. Our theoretical framework provides a fundamental principle for label-free detection using CNT resonators based on DNA–CNT interactions.

(Some figures in this article are in colour only in the electronic version)

1. Introduction

Single-walled carbon nanotubes (CNTs) and single-stranded DNA molecules are two types of one-dimensional nanostructures with comparable lateral dimensions. Recent studies show single-stranded DNA can form stable negatively charged hybrid structures with CNTs by wrapping around the CNT side surface in a helical fashion [1, 2]. The helical binding of DNA to CNT is ascribed to the formation of π stacking between nucleobases and the CNT side surface, which is also modulated by the repulsive electrostatic interactions between negative charges on the phosphate group of the DNA backbone [3]. The DNA–CNT hybrids provide an innovative venue for nanoscale manipulation of DNA and CNTs, such as CNT sorting, separation [1, 2] and patterned placement [4], DNA transportation and thermal ablation treatment [5]. Moreover, CNTs have recently received a lot of attention for their applications as mechanical resonators, which exhibit high-frequency dynamic ranges [6, 7] due to their high Young's modulus and low density properties [8]. The CNT-based high-frequency resonators have been employed for label-free detection of various molecules based on the resonant frequency shift upon molecular binding and/or adsorption [9–11]. A recent study by Zettl and his coworkers [12] suggests the potential of CNTs as resonators for

label-free detection of chemical molecules with a resolution of a few atoms. Their results indicate that theoretical characterization of resonance behaviour of CNTs is essential for their sensing applications. Only very recently, theoretical models based on the continuum mechanics were developed for the characterization of the resonance behaviour of CNTs [13, 14]. Coarse-grained models were also employed for the characterization of the resonant frequency shift of CNTs in response to mass adsorption [15]. However, the resonance behaviour of CNTs in response to biomolecular binding is little explored, although CNT-based resonators hold the potential as sensors for the detection of biomolecules such as DNA and/or proteins.

In this study, we theoretically investigate the role of the helically wrapped DNA on the dynamical response of CNTs in an aqueous environment based on a continuum model of CNT–DNA hybrid structures. Considering the CNT as a mechanical resonator, the binding of DNA introduces three factors which affect the resonance of the CNT: (1) the increase in the dynamical mass, (2) adhesion interactions between DNA nucleobases and the CNT side surface and (3) electrostatic repulsion between negative charges on the DNA backbone. The DNA–CNT adhesion is primarily driven by van der Waals interactions and hydrophobic interactions between DNA nucleobases and CNT. Previous studies have shown that the adhesion strength is nucleobase dependent [16–23]. For instance, if we consider the binding energy between individual nucleobase and CNT, the binding energy for adenines is stronger than that for thymines. However, if we consider their homopolymer chains, i.e. polydeoxyadenylate (poly(dA)) and deoxythymidylate (poly(dT)), the effective binding energy per base for poly(dT) is actually higher than that for poly(dA) [16]. This is attributed to the fact that poly(dA) forms a more orderly single-helical structure as a result of strong base-stacking interactions between neighbouring adenines [24, 25], while poly(dT) stays in a random-coil conformation with little or no base-stacking interaction between thymines [26, 27]. Therefore, it is more readily for a poly(dT) chain to form π stacking with CNT than a comparable poly(dA) chain, because the adhesion interactions for the latter have to compete with the stacking interactions. The helical wrapping of the DNA on the CNT is also modulated by the electrostatic repulsion between negative charges on the DNA backbone. From an energy point of view, the DNA helical wrapping reaches its preferred or equilibrium state when the potential energy including both the adhesion and electrostatic energies reaches a minimum. Regarding the dynamical response of the DNA–CNT hybrid, the electrostatic interaction will vary when the DNA–CNT hybrid is under a bended configuration compared with its unbended configuration because the distance between the charges on the DNA backbone depends on the bending curvature. The variation of the electrostatic energy will alter the repulsive electrostatic force applied to the CNT, and thus affect the CNT's dynamic behaviours, such as its resonant frequency. The rest of this paper is organized as follows: in section 2, we present a continuum model of DNA–CNT hybrids, and analyse the equilibrium configuration of helical wrapping of DNA on CNT. On that basis, we study the resonance response of CNT to binding of DNA (e.g. poly(dT) or poly(dA)) based on the variational method with a Hamiltonian, which takes into account the CNT bending energy as well as the interaction energy driven by DNA wrapping. Section 3 presents the numerical results of the equilibrium configuration and the resonance behaviour of DNA–CNT hybrids. Finally, our study is summarized in section 4.

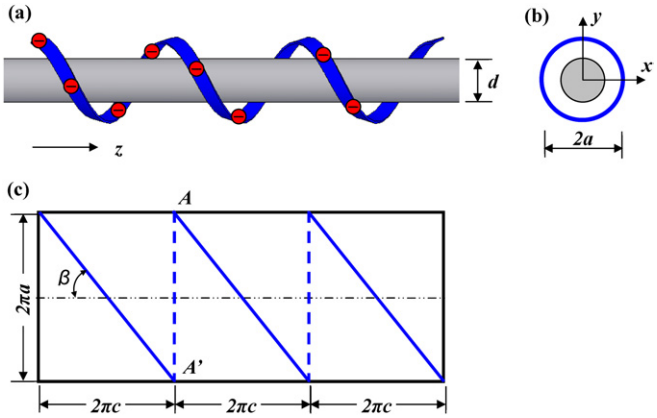

Figure 1. Schematics of the CNT–DNA hybrid structure: (*a*) front view; (*b*) side view; (*c*) expansion view of the DNA helix in (*a*) (solid line). End positions of the dotted line such as A and A′ represent the same point on the DNA helix in (*a*).

2. Modeling

2.1. Equilibrium binding configuration of DNA–CNT hybrids

In order to find out the resonance behaviour of the CNT in response to the DNA–CNT interactions, we need to first obtain the equilibrium helical configuration for the DNA binding to the CNT, which results from the competition between the binding interaction between the CNT and the DNA chain and the electrostatic interaction between electric charges on the DNA chain. On the other hand, the confinement of the DNA on the CNT will also affect the electrostatic interaction as the distance between electrical charges is likely to change. In our model, which is schematically shown in figure 1, the CNT is considered as a uniform and dielectric rod of length L and diameter d, which is valid for single-walled CNTs with large band-gap [28], while the DNA is considered as a continuous uniform flexible belt helically wrapped around the CNT side surface with evenly distributed negative electrical charges. The helical configuration of the DNA on the CNT surface is described by rotation angle t. The rotation angle interval Δt per nucleotide is given by $\Delta t = \lambda/\sqrt{a^2+c^2} = \lambda/a(1+(\tan(\beta))^{-2})^{-1/2}$, in which λ is the nucleotide length ($\lambda = 0.7$ nm for both dA and dT), a is the radius of the DNA helix, c is the helix pitch and β is the DNA helical wrapping angle. Now, let us consider two randomly selected electrical charges (mth and nth sites) on the DNA chain whose coordinates are $x_k = a\cos(k\Delta t)$, $y_k = a\sin(k\Delta t)$ and $z_k = ck\Delta t$ ($k = m$ or n), and the resulting vector $\boldsymbol{r}_{mn}$ formed by these two charge sites. The total electrostatic energy in the DNA chain which is composed of N nucleotides in total is

given by

$$E_{\text{elec}} = \sum_{n=1}^{N-1} \sum_{m=n+1}^{N} \frac{q^2}{4\pi \langle \varepsilon_{mn} \rangle r_{mn} \varepsilon_0}, \tag{1}$$

where $q = 1.602 \times 10^{-19}$ C is the electrical charge carried by one electron, $\varepsilon_0 = 8.854 \times 10^{-12}\,\text{C}^2\,\text{N}^{-1}\,\text{m}^{-2}$ is the vacuum permittivity, $r_{mn} = |\boldsymbol{r}_{mn}|$ is the distance between the mth and the nth charges and $\langle \varepsilon_{mn} \rangle$ is the average permittivity constant given by

$$\langle \varepsilon_{mn} \rangle = \frac{\varepsilon_{\text{CNT}} l_{\text{c}} + \varepsilon_{\text{water}} (r_{mn} - l_{\text{c}})}{r_{mn}}, \tag{2}$$

where $\varepsilon_{\text{CNT}} = 10$ and $\varepsilon_{\text{water}} = 80$ are the permittivity coefficients for CNTs (considered as graphite) and water, respectively, and l_{c} is the length of the portion of the vector $\boldsymbol{r}_{mn}$ inside the CNT cylinder. It is noted that, for simplicity, our model does not take into account counter-ions [16, 29] (such as Na^+) in the typical DNA buffer solution in the calculation of the electrostatic energy. The existence of counter-ions will reduce the effective charges on the DNA backbones and therefore weaken the electrostatic interactions between DNA nucleotides, indicating that the electrostatic energy predicted by equation (1) is, to some extent, overestimated.

The binding energy between the CNT and the DNA chain is given by

$$E_{\text{bind}} = -N\mu, \tag{3}$$

where μ is the binding energy between the nucleobase and the CNT. The equilibrium helical wrapping configuration can be found from minimizing the potential energy *per unit CNT length* with respect to the wrapping angle, i.e. $\partial((E_{\text{elec}} + E_{\text{bind}})/N\lambda \cos\beta)/\partial\beta = 0$. This leads to the finding of the wrapping angle β in the equilibrium helical binding configuration.

In our study, the DNA chain is assumed to bind the CNT in a helical fashion. A very recent molecular dynamics simulation study by Johnson *et al* [21] interestingly reveals that DNA may take non-helical wrapping configurations in DNA–CNT complexes, such as U-shaped loops. In order to predict the equilibrium binding configuration for such non-helical DNA–CNT hybrids, our model has to be carefully revised to take into account the respective non-helical binding shape of the DNA.

2.2. Bending of DNA–CNT hybrids

When the DNA–CNT hybrid undergoes a small or linear bending motion, as illustrated in figure 2, we can reasonably consider the adsorbed nucloebases on the CNT surface with zero mobility if the resonant frequency of the CNT is assumed to be much higher than the mechanical response of the DNA chain to the electrostatic repulsive and the adhesion interactions. The positions of the electrical charges on sites m and n become m' and n' in the bended configuration as shown in figure 2. Their distance in the bended configuration is given by

$$r_{m'n'} = \sqrt{(x_{n'} - x_{m'})^2 + (y_{n'} - y_{m'})^2 + (z_{n'} - z_{m'})^2}, \tag{4a}$$

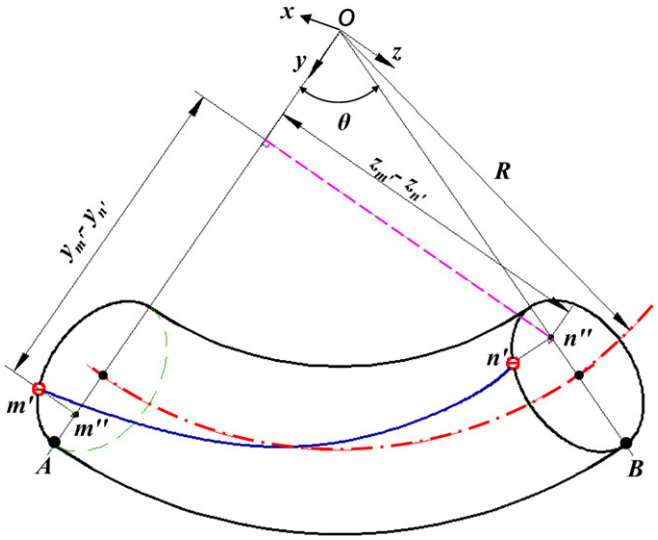

Figure 2. Schematic of the deformed CNT–DNA hybrid structure. m'' and n'' are the projection of m' and n' on the curvature plane OAB, respectively.

where

$$\begin{aligned} x_{n'} - x_{m'} &= x_n - x_m, \\ y_{n'} - y_{m'} &= (R - y_n)\cos\theta - (R - y_m), \\ z_{n'} - z_{m'} &= (R - y_n)\sin\theta. \end{aligned} \tag{4b}$$

Here, the prime indicates the bended configuration, $1/R$ or κ is the curvature for the bended CNT–DNA complex (i.e. $\kappa = 1/R = \partial^2 w(z, t)/\partial z^2$, where $w(z, t)$ is the bending deflection) and angle θ is given as $\theta = \kappa(z_n - z_m)$. It is noted that the binding energy between the DNA chain and the CNT is independent of curvature κ in the bended configuration. From equations (4*a*) and (4*b*), the distance between electrical charges in the bended DNA–CNT complex can be rewritten as

$$r_{m'n'} = r_{mn}\sqrt{1 - P_{mn}\kappa + Q_{mn}\kappa^2}, \tag{5}$$

where P_{mn} and Q_{mn} are defined as $P_{mn} = ac^2(\Delta t)^2(m-n)^2 (\sin(m\Delta t) + \sin(n\Delta t))/r_{mn}^2$ and $Q_{mn} = a^2c^2(\Delta t)^2(m-n)^2 \sin(m\Delta t)\sin(n\Delta t)/r_{mn}^2$, respectively. The electrostatic energy in the bended configuration can be approximated by

$$\begin{aligned} E_{\text{elec}} &\approx \sum_{n=1}^{N-1} \sum_{m=n+1}^{N} \frac{q^2}{4\pi \langle \varepsilon_{mn} \rangle r_{mn}} \left(1 - P_{mn}\kappa + Q_{mn}\kappa^2\right)^{-1/2} \\ &= \sum_{n=1}^{N-1} \sum_{m=n+1}^{N} \frac{q^2}{4\pi \langle \varepsilon_{mn} \rangle r_{mn}} \left[1 + \frac{P_{mn}}{2}\kappa \right. \\ &\quad \left. + \left(\frac{3}{8}P_{mn}^2 - \frac{Q_{mn}}{2}\right)\kappa^2 + O\left(\kappa^3\right)\right]. \end{aligned} \tag{6}$$

In equation (6), for simplicity, we assume that the average permittivity in the bended configuration can be approximated by that of the unbended configuration. The total potential energy U for the DNA–CNT complex consists of the bending energy of the CNT and the electrostatic interaction among

electrical charges on the DNA, and is given by

$$U = \int_0^L \frac{(\mathrm{EI})_0}{2}\kappa^2 \mathrm{d}z + \sum_{n=1}^{N-1}\sum_{m=n+1}^{N} \frac{q^2}{4\pi\,\langle\varepsilon_{mn}\rangle\, r_{mn}} \times \left[1 + \frac{P_{mn}}{2}\kappa + \left(\frac{3}{8}P_{mn}^2 - \frac{Q_{mn}}{2}\right)\kappa^2\right] = \int_0^L \left[\xi + \psi\kappa + \frac{(\mathrm{EI})_0 + \eta}{2}\kappa^2\right]\mathrm{d}z, \quad (7)$$

where $(\mathrm{EI})_0$ is the bending modulus of the CNT, and three newly introduced parameters (ξ, ψ, η) are given as

$$\xi = \frac{1}{L}\left(\sum_{n=1}^{N-1}\sum_{m=n+1}^{N} \frac{q^2}{4\pi\,\langle\varepsilon_{mn}\rangle\, r_{mn}}\right),$$

$$\psi = \frac{1}{L}\left(\sum_{n=1}^{N-1}\sum_{m=n+1}^{N} \frac{q^2 P_{mn}}{8\pi\,\langle\varepsilon_{mn}\rangle\, r_{mn}}\right), \quad (8)$$

$$\eta = \frac{1}{L}\left(\sum_{n=1}^{N-1}\sum_{m=n+1}^{N} \frac{q^2}{4\pi\,\langle\varepsilon_{mn}\rangle\, r_{mn}}\left(\frac{3}{4}P_{mn}^2 - Q_{mn}\right)\right).$$

The kinetic energy T for the CNT–DNA complex is given by

$$T = \int_0^L \frac{1}{2}\left(\mu_{\mathrm{CNT}} + \mu_{\mathrm{hydro}} + \mu_{\mathrm{DNA}}\zeta\sqrt{1+\tan^2\beta}\right) \times \left(\frac{\partial w}{\partial t}\right)^2 \mathrm{d}z, \quad (9)$$

where μ_{CNT}, μ_{hydro} and μ_{DNA} represent the masses per unit length for CNT, hydrodynamic loading and DNA molecule, respectively, and $\zeta(z) = 0$ or 1 is a quantity indicating the presence of the nucleobase on the CNT surface. The hydrodynamic loading effect arises from the aqueous environment which surrounds the CNT resonator [30–33]. Previous studies [32, 33] suggest that the hydrodynamic loading effect plays a more prominent role than the damping effect in determining the resonance behaviour of CNTs in aqueous environments. The hydrodynamic loading coupled to the resonance behaviour of the CNT can be estimated by [30–33]

$$\frac{\mu_{\mathrm{hydro}}}{\mu_{\mathrm{CNT}}} = \left(1 + \frac{4L}{\beta_{\mathrm{r}} d^2\sqrt{\omega_{\mathrm{n}}/\nu}}\right)\left(\frac{\rho_{\mathrm{water}}}{\rho_{\mathrm{CNT}}}\right), \quad (10)$$

where β_{r} is a constant to satisfy the transcendental equation arising from the CNT boundary conditions, ω_{n} is the natural frequency of the CNT given by $\omega_{\mathrm{n}} = (\beta_{\mathrm{r}}/L)^2((\mathrm{EI})_0/\mu_{\mathrm{CNT}})^{1/2}$, ν is the kinetic viscosity of water at room temperature ($\nu = 10^{-6}\,\mathrm{m^2\,s^{-1}}$), $\rho_{\mathrm{water}} = 1\,\mathrm{g\,cm^{-3}}$ and $\rho_{\mathrm{CNT}} = 1.35\,\mathrm{g\,cm^{-3}}$ are the densities of water and CNT, respectively, and d and L represent the cross-sectional diameter and length of the CNT, respectively. The resonant frequency of the CNT cantilever in water is given by $\omega_{\mathrm{r}} = \omega_{\mathrm{n}}(1 + \mu_{\mathrm{hydro}}/\mu_{\mathrm{CNT}})^{-1/2}$.

For an oscillating system, the deflection $w(z, t)$ can be written in the form of $w(z, t) = u(z)\exp[\mathrm{i}\omega t]$, where ω and $u(z)$ are the resonant frequency and its corresponding deflection eigen-mode, respectively. The Hamiltonian H of the CNT–DNA complex per oscillation cycle becomes

$$H = -\frac{\omega^2}{2}\int_0^L \left(\mu_{\mathrm{CNT}} + \mu_{\mathrm{hydro}} + \mu_{\mathrm{DNA}}\zeta\sqrt{1+\tan^2\beta}\right)u^2\mathrm{d}z + \int_0^L \left[\xi + \psi\left(\frac{\mathrm{d}^2u}{\mathrm{d}z^2}\right) + \frac{(\mathrm{EI})_0 + \eta}{2}\left(\frac{\mathrm{d}^2u}{\mathrm{d}z^2}\right)^2\right]\mathrm{d}z. \quad (11)$$

The variational method allows for obtaining the equation of motion

$$-\omega^2\left[\mu_{\mathrm{CNT}} + \mu_{\mathrm{hydro}} + \left(\mu_{\mathrm{DNA}}\sqrt{1+\tan^2\beta}\right)\cdot\zeta(z)\right]u(z) + \left[(\mathrm{EI})_0 + \eta\right]\left(\frac{\mathrm{d}^4u}{\mathrm{d}z^4}\right) = 0. \quad (12)$$

Now let us consider the Rayleigh–Ritz method in order to find the resonant frequency $\omega_{\mathrm{r}}^{\mathrm{dcc}}$ of the DNA–CNT complex (dcc). The Rayleigh quotient R is defined as [34]

$$R = \frac{\int_0^L \left[(\mathrm{EI})_0 + \eta\right]\left(\frac{\mathrm{d}^2v}{\mathrm{d}z^2}\right)^2\mathrm{d}z}{\int_0^L \left[\mu_{\mathrm{CNT}} + \mu_{\mathrm{hydro}} + \left(\mu_{\mathrm{DNA}}\sqrt{1+\tan^2\beta}\right)\cdot\zeta(z)\right](v(z))^2\,\mathrm{d}z}, \quad (13)$$

where $v(z)$ is the admissible function that satisfies the essential boundary conditions. If the admissible function is close to the deflection eigen-mode $u(z)$, then the Rayleigh quotient [34] approaches the square of resonant frequency of the DNA–CNT hybrid, i.e. $R^{1/2} \approx \omega_{\mathrm{r}}^{\mathrm{dcc}}$. To find the resonant frequency, the deflection shape of the CNT is assumed to follow a fourth-order polynomial. For a cantilevered CNT, the normalized admissible function $v(z)$ is given by [35]

$$v(z) = \sqrt{\frac{45}{104L}}\left(6\left(\frac{z}{L}\right)^2 - 4\left(\frac{z}{L}\right)^3 + \left(\frac{z}{L}\right)^4\right). \quad (14)$$

Here, it is noted that $v(z)$ satisfies the essential cantilever boundary conditions, i.e. $v(0) = v'(0) = 0$, and $v''(L) = v'''(L) = 0$ and $\int_0^L [v(z)]^2\mathrm{d}z = 1$.

From equation (13), the normalized resonant frequency of the DNA–CNT complex can be obtained as

$$\frac{\omega_{\mathrm{r}}^{\mathrm{dcc}}}{\omega_{\mathrm{n}}} = \left(\frac{L}{\beta_r}\right)^2\left\{\left[\int_0^L [1 + (\eta/(\mathrm{EI})_0)]\left(\mathrm{d}^2v/\mathrm{d}z^2\right)^2\,\mathrm{d}z\right] \times \left[\int_0^L \left[1 + (\mu_{\mathrm{hydro}}/\mu_{\mathrm{CNT}}) + \left((\mu_{\mathrm{DNA}}/\mu_{\mathrm{CNT}})\sqrt{1+\tan^2\beta}\right)\cdot\zeta(z)\right](v(z))^2\,\mathrm{d}z\right]^{-1}\right\}^{\frac{1}{2}}. \quad (15)$$

If we consider a DNA chain with its length much smaller than the CNT length, equation (15) can be approximated by

$$\frac{\omega_{\mathrm{r}}^{\mathrm{dcc}}}{\omega_{\mathrm{r}}} \approx \sqrt{\frac{(1 + (\eta/(\mathrm{EI})_0))}{1 + (\mu_{\mathrm{DNA}}N\lambda/(\mu_{\mathrm{CNT}} + \mu_{\mathrm{hydro}}))\,[v(z_{\mathrm{DNA}})]^2}}, \quad (16)$$

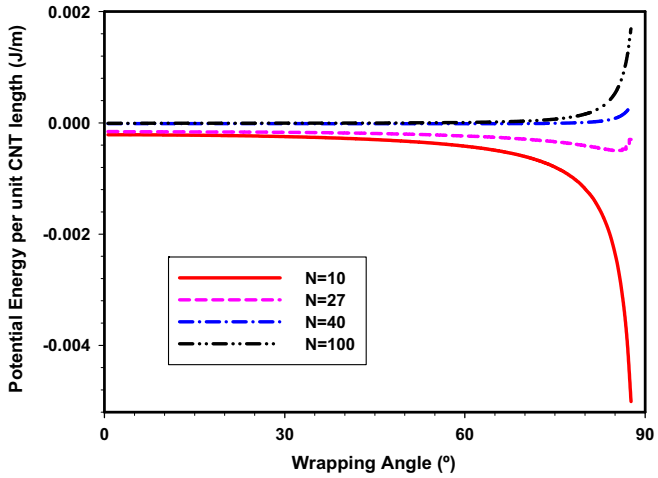

Figure 3. The dependence of the potential energy of the poly(dT)–CNT structure per unit CNT length on the helical wrapping angle for four different DNA lengths.

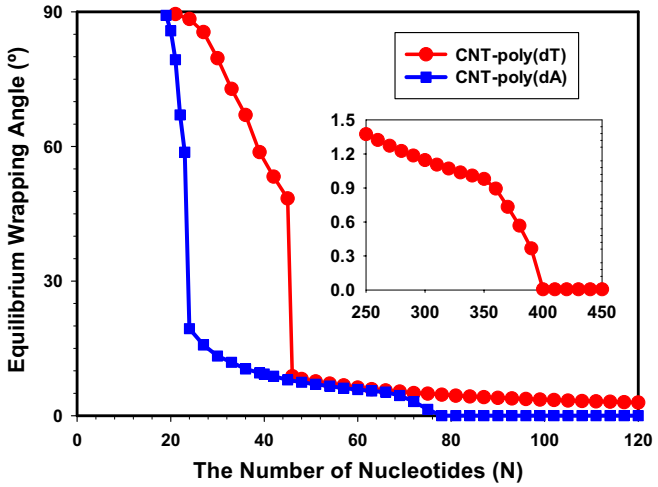

Figure 4. The dependence of the equilibrium helical wrapping angles on DNA length for both poly(dA) and poly(dT).

where z_{DNA} is the midpoint position of the DNA along the CNT. It can be easily seen that the resonant frequency shift due to the DNA binding onto the CNT is attributed to the electrostatic interaction represented by $\eta/(EI)_0$ and the mass effect of DNA, μ_{DNA}. It is noted that equations (15) and (16) are also valid for the CNT in the fixed-fixed beam configuration provided that an admission function $v(z)$ satisfying the fixed-fixed boundary conditions is used.

3. Result and discussion

We consider the following parameters in the simulations: dT and dA have molecular weights of 305.901 Da and 314.911 Da, respectively. The effective adhesion energy for dT-CNT is 3.3 kcal mol^{-1}, while 2.32 kcal mol^{-1} for dA-CNT [16]. It is noted that these values already take into account the percentage of thymine or adenine bases which are not in π stacking with the CNT surface. The diameter of the single-walled CNT is assumed to be 2 nm and the lateral distance between the DNA and the CNT or the distance between DNA phosphate atoms and the CNT side surface is considered to be 1 nm [16]. These parameters are used for all the simulations and discussion in this paper, unless otherwise specified.

We first examine the equilibrium helical wrapping configuration of poly(dT) and poly(dA) on the CNT. Figure 3 shows the dependence of the potential energy of the poly(dT)–CNT structure per unit CNT length on the helical wrapping angle for four different DNA lengths. Three groups of behaviours are identified. When the DNA is very short (i.e. $N = 10$, as shown in figure 3), the electrostatic interactions among charges on the DNA backbone is weak compared with the binding energy. The binding energy between nucleobases and the CNT plays a dominant role in determining the DNA helical wrapping configuration. As shown by the solid curve in figure 3, no potential well exists for such a case and the wrapping angle $\beta - > 90^\circ$ for minimum potential energy (per unit CNT length) because the electrostatic interaction becomes strongest at $\beta = 90^\circ$ and the corresponding spanning length of the DNA in the CNT length direction approaches zero. With the increase in DNA length (i.e. $N = 27$ and 40 as shown in figure 3), the potential energy curve indeed displays a potential well with its minimum corresponding to the equilibrium helical wrapping angles of 85° and 57°, respectively, for the aforementioned two cases. Our results clearly show the trend that the equilibrium helical wrapping angle becomes smaller with the increase in DNA length. It is found that the equilibrium wrapping angle decreases to 3.5° when $N = 100$ (the dash-dot-dot curve in figure 3). This is due to the fact that the electrostatic energy increases more rapidly than the binding energy with the increase in DNA length. This behaviour is also clearly illustrated in figure 4, which shows the equilibrium helical wrapping angle as a function of DNA length (i.e. the number of nucleotides N) for both poly(dT) and poly(dA). Figure 4 interestingly displays similar sharp transitions in the wrapping angle-DNA length profile for both poly(dT)–CNT and poly(dA)–CNT complexes. We believe that this observed transition represents different binding mechanisms arising from the competition between the adhesion and the electrostatic repulsion. Specifically, for a short DNA chain, the binding energy (adhesion energy) plays a key role in the DNA binding mechanism onto CNT, while the electrostatic repulsion becomes a dominant factor for the binding of a long DNA chain onto CNT. The transitions take place at $N = 46$ for poly(dT) and $N = 24$ for poly(dA), respectively. The angular change in this sharp transition is approximately 39° for both molecules. This result importantly indicates that the equilibrium helical wrapping configuration does not exist for a certain angular range. Because the effective binding energy for dT is higher than that for dA, the equilibrium helical binding angle for poly(dT) is larger than that for comparable poly(dA). For poly(dA), β gradually decreases from 19.40° for $N = 24$ to 4.5° for $N = 69$, then drops rapidly to zero for $N = 78$, indicating the electrostatic repulsive interactions between DNA nucleobases cannot be balanced by the adhesion interaction. For $N \geqslant 78$, the DNA chain is likely in a straight line configuration on the surface of the CNT, which minimizes the electrostatic interactions between

charges. The preferred wrapping angle-DNA length profile of poly(dT) displays a similar pattern as that of poly(dA), but β in the former declines at a much slower pace, as shown in figure 4. For poly(dT), our results show that β drops from 8.8° for $N = 46$ to 1.0° for $N = 350$, then reaches zero at $N = 400$, as shown by the inset of figure 4. In addition, figure 4 interestingly reveals that the difference between the equilibrium wrapping angles for these two molecules of the same length is quite small (<1°) for N in the range between 46 and 69. This observation suggests that the dependence of the equilibrium wrapping angle on the effective binding energy is modulated by DNA length. It is likely that, for $46 \leqslant N \leqslant 69$, the preferred wrapping angle is less sensitive to the variation of the DNA binding energy, compared with shorter DNA, i.e. $21 \leqslant N \leqslant 45$, of which the equilibrium wrapping angle curves display much larger deviations between poly(dA) and poly(dT). It is noted that in the above analysis, we ignore the lateral dimension (i.e. the width and thickness) of the nucleotide, which will pose an additional constraint in the DNA helical binding configuration. For instance, if we assume the width of the DNA nucleotides is 0.5 nm and no overlapping between nucleobases in the helical binding configuration, we can obtain easily, from figure 1, that $\beta < 90° - \tan^{-1}(\pi/8)$.

Regarding the resonance behaviour of the DNA–CNT complex, we consider DNA–CNT complexes consisting of a poly(dT) or poly(dA) homopolyer chain with $N = 60$ and a nanotube cantilever with a length of 500 nm. The natural frequency of the CNT cantilever in vacuum is 37.2 MHz. The hydrodynamic loading on the CNT is obtained as $\mu_{\text{hydro}} = 1.3 \times 10^4 \mu_{\text{CNT}}$. The resonant frequency of the CNT cantilever in water without DNA binding is found to be only 326 KHz, representing a significant reduction in resonant frequency due to the hydrodynamic loading effect. The corresponding equilibrium helical wrapping angles can be obtained from figure 4 and are 6.25° for poly(dT) and 5.82° for poly(dA), respectively. If we examine the effects of the electrostatic interaction in the DNA chain without considering the DNA mass, the resulting resonant frequency shifts from the resonance frequency of the CNT in water can be obtained from equation (16) by considering $\mu_{\text{DNA}} = 0$, and are found to be 1.83 Hz for poly(dT) and 1.82 Hz for poly(dA), respectively. The almost identical resonance frequency shift is attributed to the similar equilibrium helical wrapping angle for both molecules at such length. We also calculate the resonance frequency shift caused by the electrostatic interaction without considering the hydrodynamic loading effect. Our results show that the resonant frequency shifts are 208 Hz for poly(dT) and 207 Hz for poly(dA), respectively. Therefore, the effect of the electrostatic interactions on the resonance behaviours of the DNA–CNT is significantly attenuated by the hydrodynamic loading effect in aqueous environments. It is noted that those resonant frequency shifts caused by the electrostatic interaction are positive (i.e. $\eta > 0$) and independent of the binding location of the DNA segment on the CNT.

By taking into account the DNA mass, the resonant response of the CNT cantilever in response to the respective poly(dT) and poly(dA) binding are obtained using equation (15) and are presented in figures 5. Figures 5(*a*) and (*b*) show the normalized resonance frequency shifts of the CNT cantilever upon DNA binding with and without considering the hydrodynamic loading effect, respectively. Our results show that the resonant response of the CNT to DNA–CNT interactions is dependent on the location of the DNA chain on the CNT, with more prominent effects when the DNA stays closer to the free end of the CNT cantilever. Our results also reveal that the role of the DNA dynamic mass in the resonance behaviour of the DNA–CNT complex is strongly impacted by the hydrodynamic loading effect. Specifically, with the consideration of the hydrodynamic loading effect, the role of the DNA dynamic mass in the resonance behaviour of the DNA–CNT complex is comparable to that of the electrostatic interactions, as shown by figure 5(*a*), while the DNA dynamic mass plays a more prominent role in determining the resonant frequency of the DNA–CNT complex than the electrostatic interactions when the hydrodynamic loading effect is omitted in the simulation (i.e. considering $\mu_{\text{hydro}} = 0$ in equation (15)), as shown in figure 5(*b*). Similarly, the resonant frequency shift difference between the bindings of these two DNA molecules to CNT, a key parameter for label-free detection of biomolecules, is also greatly impacted by the hydrodynamic loading effect, as shown in figures 5(*c*) and (*d*). Our results reveal that when the hydrodynamic loading effect is considered, the resonance frequency difference between these two DNA–CNT complexes is significantly less than 1 Hz, implying that this tiny frequency difference practically cannot be distinguished by frequency measurements. However, the resonance frequency difference is significantly higher if the hydrodynamic loading effect is omitted. For instance, the resonant frequency difference between the aforementioned two DNA–CNT complexes is calculated to be 23.1 KHz if the midpoints of DNA segments stay 400 nm away from the CNT clamped end. Therefore, for such a case, the dependence of the resonance frequency of the CNT–DNA hybrid on DNA base can be readily captured through frequency measurements. Moreover, the effect of boundary conditions on the resonant frequency shift driven by DNA binding onto the CNT can be easily recognized from equation (16). For a DNA chain of very short length compared with the CNT, we take into account two extreme cases: (i) DNA binding onto the clamped end of the CNT and (ii) DNA binding onto the free end of the CNT. The resonant frequency shift due to DNA mass can be approximated, from equation (16), as

$$\Delta\omega_{\text{r}}^{\text{dcc}}(z_{\text{DNA}}) \approx -\frac{\mu_{\text{DNA}} N\lambda[v(z_{\text{DNA}})]^2}{2(\mu_{\text{CNT}} + \mu_{\text{hydro}})}\omega_{\text{r}}.$$

For case (i), i.e. $z_{\text{DNA}} = 0$, the resonant frequency shift becomes $\Delta\omega_{\text{r}} = 0$ because of $v(0) = 0$, while for case (ii) the resonant frequency shift reaches the maximum. This indicates that the resonant frequency shift induced by DNA binding onto CNT is also dependent on the boundary conditions. This sheds lights on using CNT resonators for sensitive label-free detection of DNA molecules.

It is noted that the analysis presented in this paper regarding the dynamic response of the DNA–CNT complex focuses on two major interactions: adhesion and electrostatic interactions, while it neglects other factors such as the DNA entropic elasticity and the enthalpy increase due to

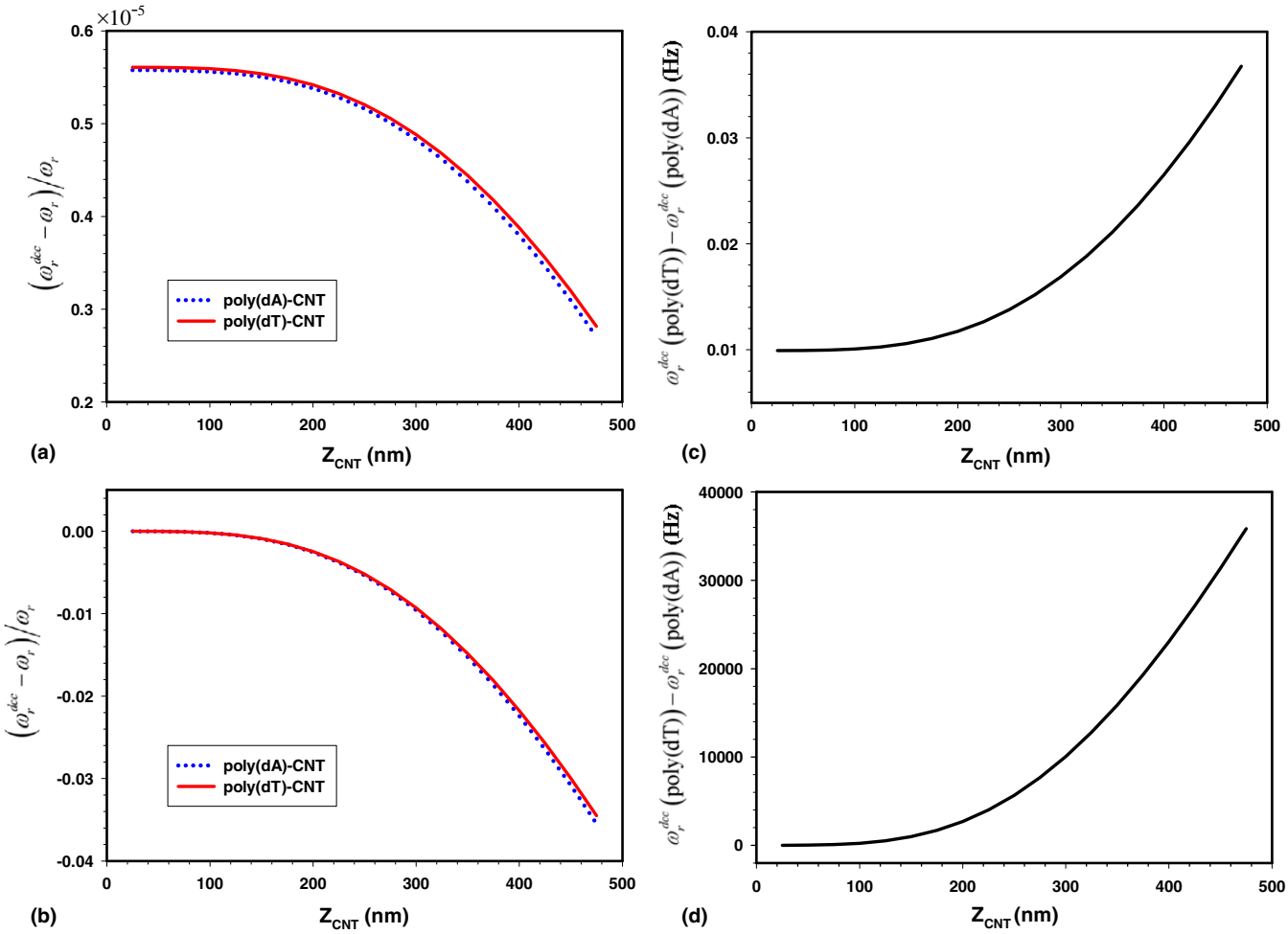

Figure 5. (*a*) and (*b*) The normalized resonance frequency shift as a function of the binding location of the DNA segment on the cantilevered CNT. (*c*) and (*d*) The resonance frequency difference between the binding of poly(dT) and poly(dA) to the CNT. The hydrodynamic loading effect is *considered* in the results shown in plots (*a*) and (*c*), while it is *omitted* in the results shown in plots (*b*) and (*d*).

the deformed CNT–DNA hybrid, which are considered to play negligible roles in determining the DNA helical binding configuration on CNT [16]. Similarly, the omission of counter-ions in the current model is expected to have negligible impacts on the resonant response of the CNT to the binding of DNA.

4. Conclusion

In this work, we study the dynamical behaviour of DNA–CNT hybrids by considering the adhesion and electrostatic interactions between CNT and two types of single-stranded DNA homopolymer chains, i.e. poly(dA) and poly(dT). The equilibrium DNA helical wrapping angle originates from the competition between the adhesion and electrostatic interactions and is obtained using the minimum potential energy method. Our results show that the DNA wrapping angle is dependent on both DNA length and DNA nucleobase, and interestingly reveal a sharp transition in the wrapping angle-DNA length profile. The resonant response of the DNA–CNT complex is analysed based on the variational method with a Hamiltonian, which considers the CNT bending energy, the electrostatic interaction variation arising from DNA binding onto the CNT. Furthermore, the closed-form analytical solution for predicting the resonant frequency of the DNA–CNT complex is presented. Our results show that the hydrodynamic loading on CNT resonators in aqueous environments has profound impacts on the resonance behaviour of DNA–CNT complexes. Our results reveal that the dependence of the resonant frequency of the DNA–CNT complex on DNA base is significantly attenuated by the hydrodynamic loading effect and is probably indistinguishable to frequency measurements in aqueous environments. Our results suggest that the detection of DNA molecules using CNT resonators based on DNA–CNT binding interaction through frequency measurements should be conducted in low hydrodynamic loading media, such as air and water vapour. The results reported in this paper are useful for understanding the resonant behaviour of DNA–CNT hybrids and provide the fundamental principle for label-free detection of DNA molecules using CNT resonators.

Acknowledgments

This work is supported by the State University of New York at Binghamton. KE acknowledges financial support by the Korea Research Foundation (Grant No KRF-2009-007-1246).

References

[1] Zheng M, Jagota A, Semke E D, Diner B A, Mclean R S, Lustig S R, Richardson R E and Tassi N G 2003 DNA-assisted dispersion and separation of carbon nanotubes *Nature Mater.* **2** 338–42

[2] Zheng M *et al* 2003 Structure-based carbon nanotube sorting by sequence-dependent DNA assembly *Science* **302** 1545–8

[3] Wall A and Ferreira M S 2006 Electronic contribution to the energetics of helically wrapped nanotubes *Phys. Rev.* B **74** 233401

[4] McLean R S, Huang X Y, Khripin C, Jagota A and Zheng M 2006 Controlled two-dimensional pattern of spontaneously aligned carbon nanotubes *Nano Lett.* **6** 55–60

[5] Kam N W S, O'Connell M, Wisdom J A and Dai H J 2005 Carbon nanotubes as multifunctional biological transporters and near-infrared agents for selective cancer cell destruction *Proc. Natl Acad. Sci. USA* **102** 11600–5

[6] Sazonova V, Yaish Y, Ustunel H, Roundy D, Arias T A and McEuen P L 2004 A tunable carbon nanotube electromechanical oscillator *Nature* **431** 284–7

[7] Witkamp B, Poot M and van der Zant H S J 2006 Bending-mode vibration of a suspended nanotube resonator *Nano Lett.* **6** 2904–8

[8] Qian D, Wagner G J, Liu W K, Yu M F and Ruoff R S 2002 Mechanics of carbon nanotubes *Appl. Mech. Rev.* **55** 495–533

[9] Yang Y T, Callegari C, Feng X L, Ekinci K L and Roukes M L 2006 Zeptogram-scale nanomechanical mass sensing *Nano Lett.* **6** 583–6

[10] Ilic B, Yang Y, Aubin K, Reichenbach R, Krylov S and Craighead H G 2005 Enumeration of DNA molecules bound to a nanomechanical oscillator *Nano Lett.* **5** 925–9

[11] Eom K, Kwon T Y, Yoon D S, Lee H L and Kim T S 2007 Dynamical response of nanomechanical resonators to biomolecular interactions *Phys. Rev* B **76** 113408

[12] Jensen K, Kim K and Zettl A 2008 An atomic-resolution nanomechanical mass sensor *Nature Nanotechnol.* **3** 533–7

[13] Sapmaz S, Blanter Y M, Gurevich L and van der Zant H S J 2003 Carbon nanotubes as nanoelectromechanical systems *Phys. Rev.* B **67** 235414

[14] Ustunel H, Roundy D and Arias T A 2005 Modeling a suspended nanotube oscillator *Nano Lett.* **5** 523–6

[15] Li C Y and Chou T W 2004 Mass detection using carbon nanotube-based nanomechanical resonators *Appl. Phys. Lett.* **84** 5246–8

[16] Manohar S, Tang T and Jagota A 2007 Structure of homopolymer DNA–CNT hybrids *J. Phys. Chem.* C **111** 17835–45

[17] Manohar S, Mantz A R, Bancroft K E, Hui C Y, Jagota A and Vezenov D V 2008 Peeling single-stranded DNA from graphite surface to determine oligonucleotide binding energy by force spectroscopy *Nano Lett.* **8** 4365–72

[18] Antony J and Grimme S 2008 Structures and interaction energies of stacked graphene–nucleobase complexes *Phys. Chem. Chem. Phys.* **10** 2722–9

[19] Shi X H, Yong K, Zhao Y P and Gao H J 2005 Molecular dynamics simulation of peeling a DNA molecule on substrate *Acta Mech. Sin.* **21** 249–56

[20] Sowerby S J, Cohn C A, Heckl W M and Holm N G 2001 Differential adsorption of nucleic acid bases: relevance to the origin of life *Proc. Natl Acad. Sci. USA* **98** 820–2

[21] Johnson R R, Kohlmeyer A, Johnson A T C and Klein M L 2009 Free energy landscape of a DNA–carbon nanotube hybrid using replica exchange molecular dynamics *Nano Lett.* **9** 537–41

[22] Gowtham S, Scheicher R H, Ahuja R, Pandey R and Karna S P 2007 Physisorption of nucleobases on graphene: density-functional calculations *Phys. Rev.* B **76** 033401

[23] Gowtham S, Scheicher R H, Pandey R, Karna S P and Ahuja R 2008 First-principles study of physisorption of nucleic acid bases on small-diameter carbon nanotubes *Nanotechnology* **19** 125701

[24] Ke C, Humeniuk M, Gracz H S and Marszalek P E 2007 Direct measurements of base stacking interactions in DNA by single-molecule atomic-force spectroscopy *Phys. Rev. Lett.* **99** 018302

[25] Seol Y, Skinner G M, Visscher K, Buhot A and Halperin A 2007 Stretching of homopolymeric RNA reveals single-stranded helices and base-stacking *Phys. Rev. Lett.* **98** 158103

[26] Mills J B, Vacano E and Hagerman P J 1999 Flexibility of single-stranded DNA: use of gapped duplex helices to determine the persistence lengths of poly(dT) and poly(dA) *J. Mol. Biol.* **285** 245–57

[27] Saenger W 1984 *Principles of Nucleic Acid Structure* (Berlin: Springer)

[28] Dresselhaus M S, Dresselaus G and Avouris P 2001 *Carbon Nanotubes* (Berlin: Springer)

[29] Kanduc M, Dobnikar J and Podgornik R 2009 Counterion-mediated electrostatic interactions between helical molecules *Soft Matter* **5** 868–77

[30] Kirstein S, Mertesdorf M and Schonhoff M 1998 The influence of a viscous fluid on the vibration dynamics of scanning near-field optical microscopy fiber probes and atomic force microscopy cantilevers *J. Appl. Phys.* **84** 1782–90

[31] Braun T, Barwich V, Ghatkesar M K, Bredekamp A H, Gerber C, Hegner M and Lang H P 2005 Micromechanical mass sensors for biomolecular detection in a physiological environment *Phys. Rev.* E **72** 031907

[32] Kwon T Y, Eom K, Park J H, Yoon D S, Kimc T S and Lee H L 2007 In situ real-time monitoring of biomolecular interactions based on resonating microcantilevers immersed in a viscous fluid *Appl. Phys. Lett.* **90** 223903

[33] Dareing D W, Tian F and Thundat T 2006 Effective mass and flow patterns of fluids surrounding microcantilevers *Ultramicroscopy* **106** 789–94

[34] Meirovitch L 1986 *Elements of Vibration Analysis* 2nd edn (New York: McGraw-Hill)

[35] Ke C-H 2009 Resonant pull-in of a double-sided driven nanotube-based electromechanical resonator *J. Appl. Phys.* **15** 024301